Turun yliopisto
University of Turku

ACTIVITY AND DUST ENVIRONMENT OF COMET 67P/CHURYUMOV-GERASIMENKO

Boris Zaprudin

TURUN YLIOPISTON JULKAISUJA – ANNALES UNIVERSITATIS TURKUENSIS
Sarja - ser. A I osa - tom. 583 | Astronomica - Chemica - Physica - Mathematica | Turku 2018

University of Turku

Faculty of Science and Engineering
Department of Physics and Astronomy

Supervised by

Harry J. Lehto
Docent, Adj. Professor
Tuorla Observatory, Department of Physics and Astronomy, University of Turku
Väisäläntie 20, 21500 Piikkiö
Finland

Reviewed by

Karri Muinonen
Professor
Department of Physics
University of Helsinki
Finland

Juergen Schmidt
Professor
Astronomy Research Unit
University of Oulu
Finland

Opponent

Hans Rickman
Professor Emeritus
Department of Physics and Astronomy
Uppsala University
Sweden

ISBN 978-951-29-7272-2 (PRINT)
ISBN 978-951-29-7273-9 (PDF)
ISSN 0082-7002 (Print)
ISSN 2343-3175 (Online)
Painosalama Oy - Turku, Finland 2018

Acknowledgements

I would like to thank several people and organizations for supporting me in this project. Firstly, I would like to express my gratitude to my supervisors Harry Lehto who lured me into the world of international academic research and Kari Nilsson who taught me many vital secrets of astronomical data analysis. Besides supervisors, I would like to thank my colleagues, co-authors and other contributors for creating a fruitful teamwork. Colin Snodgrass, Rita Schulz, Auni Somero, Sihane Merouane and Johan Silén have played a special role and advised me a lot during this project. I would also like to thank Esko Gardner and Silja Saarento for programming advice and proofreading the text. Approaching the finish line, I have appreciated the supportive statements of the pre-examiners of my work: Professor Karri Muinonen and Professor Juergen Schmidt. I want to thank my opponent, Professor Emeritus Hans Rickman, for agreeing to review my work at the public examination. Finally, I would like to express my gratitude to the whole scientific community, of which a special place was Tuorla Observatory. For decades, Tuorla provided the infrastructure and a unique supportive atmosphere for efficient research work, which also made this thesis possible.

Contents

Abstract

Comets are scientifically interesting objects for several reasons. Comets are among the most pristine objects of the Solar System, which can give us a way to directly study the imprints of the Solar System formation processes. Comets may have been the main mechanism for delivering volatile compounds, such as water, into the inner Solar System, including the Earth. In addition, comets contain a fair amount of complex organic material which may have descended on the primordial Earth and contributed to the emergence of life.

Ground-based observations of comets have limited capabilities. Therefore, cometary space missions were designed and performed during the last few decades. The most recent and elaborated one was the Rosetta mission, performed by the European Space Agency. This mission has provided us with a unique set of *in-situ* data, making comet 67P/C-G one of the most studied minor bodies of the Solar System. However, space missions are limited in number and by the types of objects they can reach, resulting in only few comets that were studied *in-situ*. It is, thus, extremely important to transfer the knowledge gained through the space missions to other comets which have only been observed from the ground.

In this work, an introductory review of the subject as well as four original research articles are presented. Two articles cover the activity and coma structure evolution of comet 67P/C-G during the Rosetta mission, monitored with the Nordic Optical Telescope. The other two articles present the *in-situ* data obtained with the COSIMA instrument onboard Rosetta and the analysis tools developed for the instrument. The activity of comet 67P/C-G is studied on several scales: from the individual microscopic dust particles, collected by COSIMA in the proximity of the comet's nucleus, to the global structures of the coma, reaching 10^4 kilometers, observed from the ground. These methods are complementary: the local data obtained by Rosetta are unresolvable for the ground-based telescopes, while remotely observed coma structures are not visible to Rosetta's instrumentation.

Tiivistelmä

Tieteellinen kiinnostus komeettoihin on erityisen vahvaa muutamasta syystä. Komeetat ovat parhaiten säilyneitä kappaleita Aurinkokunnassa, joten tutkimalla komeettoja voidaan jäljittää Aurinkokunnan muodostumisprosessien yksityiskohtia. Komeetoilla on todennäköisesti ollut merkitys Maapallon hydrosfäärin muodostumisessa, eli valtamertemme vesien alkuperä saattaa olla kometaarinen. Ehkä kiehtovin kiinnostuksen syy ovat komeetoissa mitatut monimuotoiset abioottiset orgaaniset aineet. Nämä aineet ovat todennäköisesti myös laskeutuneet muinaisen Maan pinnalle sekä valtamerten vesille, muodostaen sopivan kemiallisen alustan elämän synnylle.

Komeettojen tutkimus Maan pinnalta on haastavaa, joten viime vuosikymmeninä yhä näkyvämmin tulivat esille avaruusmissiot komeettoihin. Missioista viimeisin ja edistyksellisin oli Rosetta. Rosetta-avaruusluotain on seurannut komeettaa 67P/Churyumov-Gerasimenko yli kahden vuoden ajan ottaen jatkuvasti mittauksia monella tutkimuslaitteella. Rosetta-mission vuoksi komeetasta 67P/C-G on tullut ehkä tutkituin Aurinkokunnan pienkappale. Avaruusmissiot komeettoihin ovat kuitenkin harvinaisia, eivätkä kaikki komeettojen tyypit ole missioille sopivia. Tähän asti ainoastaan muutamia komeettoja on tutkittu paikan päällä, joten niistä saatujen tietojen yleistäminen muihin komeettoihin maanpäällisten havaintojen kautta on erittäin tärkeä tehtävä.

Tämä työ sisältää aihepiirin yleisen katsauksen lisäksi neljä alkuperäistä julkaisua. Kaksi julkaisua esittävät keskeiset tulokset komeetasta 67P/C-G Pohjoismaisella Optisella Kaukoputkella tehdyistä maanpäällisistä havainnoista. Kaksi muuta julkaisua kattavat Rosetta-luotaimen COSIMA-laitteen avulla saatuja mittaustuloksia sekä kehitettyjä datankäsittelymenetelmiä. Näin ollen komeettaa 67P/C-G on tutkittu eri mittakaavoissa - kooman sisuksista kerätyistä mikroskooppisista hiukkasista kymmenien tuhansien kilometrien suuruisiin kooman rakenteisiin.

List of publications

I Analysis of COSIMA spectra: Bayesian approach, *H.J. Lehto, B. Zaprudin, K. M. Lehto, T. Lönnberg, J. Silén, J. Rynö, H. Krüger, M. Hilchenbach, J. Kissel, Geosci. Instrum. Method. Data Syst., 4, 139-148, (2015).*

II Optical observations of comet 67P/Churyumov-Gerasimenko with the Nordic Optical Telescope. Comet activity before the solar conjunction, *B. Zaprudin, H.J. Lehto, K. Nilsson, T. Pursimo, A. Somero, C. Snodgrass, R. Schulz, A&A, 583, A10 (2015).*

III Dust particle flux and size distribution in the coma of 67P/Churyumov-Gerasimenko measured in situ by the COSIMA instrument on board Rosetta, *S. Merouane, B. Zaprudin, O. Stenzel, Y. Langevin, N. Altobelli, V. Della Corte, H. Fisher, M. Fulle, K. Hornung, J. Silén, N. Ligier, A. Rotundi, J. Rynö, R. Schulz, M. Hilchenbach, J. Kissel, and the COSIMA Team, A&A, 596, A87 (2016).*

IV Solar-insolation-induced changes in the coma morphology of comet 67P/Churyumov-Gerasimenko. Optical monitoring with the Nordic Optical Telescope, *B. Zaprudin, H.J. Lehto, K. Nilsson, T. Pursimo, A. Somero, C. Snodgrass, R. Schulz, A&A, 604, A3 (2017).*

Additional publications not included in the thesis

I **Comet 67P/Churyumov-Gerasimenko sheds dust coat accumulated over the past four years**, *R. Schulz, M. Hilchenbach, Y. Langevin, J. Kissel, J. Silen, C. Briois, C. Engrand, K. Hornung, D. Baklouti, A. Bardyn, H. Cottin, H. Fischer, N. Fray, M. Godard, H. Lehto, L. Le Roy, S. Merouane, F. Orthous-Daunay, J. Paquette, J. Rynö, S. Siljeström, O. Stenzel, L. Thirkell, K. Varmuza, B. Zaprudin, Nature, 518, Issue 7538, pp.216-218, (2015).*

II **Comet 67P/Churyumov-Gerasimenko: Close-up on Dust Particle Fragments**, *M. Hilchenbach, J. Kissel, Y. Langevin, C. Briois, H. von Hoerner, A. Koch, R. Schulz, J. Silén, K. Altwegg, L. Colangeli, H. Cottin, C. Engrand, H. Fischer, A. Glasmachers, E. Grün, G. Haerendel, H. Henkel, H. Höfner, K. Hornung, E. K. Jessberger, H. Lehto, K. Lehto, F. Raulin, L. Le Roy, J. Rynö, W. Steiger, T. Stephan, L. Thirkell, R. Thomas, K. Torkar, K. Varmuza, K.-P. Wanczek, N. Altobelli, D. Baklouti, A. Bardyn, N. Fray, H. Krüger, N. Ligier, Z. Lin, P. Martin, S. Merouane, F. R. Orthous-Daunay, J. Paquette, C. Revillet, S. Siljeström, O. Stenzel, B. Zaprudin, The Astrophysical Journal Letters, 816, 2, (2016).*

III **High-molecular-weight organic matter in the particles of comet 67P/Churyumov-Gerasimenko**, *N. Fray, A. Bardyn, H. Cottin, K. Altwegg, D. Baklouti, C. Briois, L. Colangeli, C. Engrand, H. Fischer, A. Glasmachers, E. Grün, G. Haerendel, H. Henkel, H. Höfner, K. Hornung, E. K. Jessberger, A. Koch, H. Krüger, Y. Langevin, H. Lehto, K. Lehto, L. Le Roy, S. Merouane, P. Modica, F.-R. Orthous-Daunay, J. Paquette, F. Raulin, J. Rynö, R. Schulz, J. Silén, S. Siljeström, W. Steiger, O. Stenzel, T. Stephan, L. Thirkell, R. Thomas, K. Torkar, K. Varmuza, K.-P. Wanczek, B. Zaprudin, J. Kissel, M. Hilchenbach, Nature, 538, 72-76, (2016).*

IV **Evolution of the physical properties of dust and cometary dust activity from 67P/Churyumov-Gerasimenko measured in situ by Rosetta/COSIMA**, *S. Merouane, O. Stenzel, M. Hilchenbach, R. Schulz, N. Altobelli, H. Fisher, K. Hornung, J. Kissel, Y. Langevin, E. Mellado, J. Rynö, B. Zaprudin, MNRAS, 469, S459-S474, (2017).*

V The 67P/Churyumov-Gerasimenko observation campaign in support of the Rosetta mission, *C. Snodgrass, M. F. A'Hearn, F. Aceituno, V. Afanasiev, S. Bagnulo, J. Bauer, G. Bergond, S. Besse, N. Biver, D. Bodewits, H. Boehnhardt, B. P. Bonev, G. Borisov, B. Carry, V. Casanova, A. Cochran, B. C. Conn, B. Davidsson, J. K. Davies, J. de León, E. de Mooij, M. de Val-Borro, M. Delacruz, M. A. DiSanti, J. E. Drew, R. Duffard, N. J. T. Edberg, S. Faggi, L. Feaga, A. Fitzsimmons, H. Fujiwara, E. L. Gibb, M. Gillon, S. F. Green, A. Guijarro, A. Guilbert-Lepoutre, P. J. Gutiérrez, E. Hadamcik, O. Hainaut, S. Haque, R. Hedrosa, D. Hines, U. Hopp, F. Hoyo, D. Hutsemékers, M. Hyland, O. Ivanova, E. Jehin, G. H. Jones, J. V. Keane, M. S. P. Kelley, N. Kiselev, J. Kleyna, M. Kluge, M. M. Knight, R. Kokotanekova, D. Koschny, E. A. Kramer, J. J. López-Moreno, P. Lacerda, L. M. Lara, J. Lasue, H. J. Lehto, A. C. Levasseur-Regourd, J. Licandro, Z. Y. Lin, T. Lister, S. C. Lowry, A. Mainzer, J. Manfroid, J. Marchant, A. J. McKay, A. McNeill, K. J. Meech, M. Micheli, I. Mohammed, M. Monguió, F. Moreno, O. Muñoz, M. J. Mumma, P. Nikolov, C. Opitom, J. L. Ortiz, L. Paganini, M. Pajuelo, F. J. Pozuelos, S. Protopapa, T. Pursimo, B. Rajkumar, Y. Ramanjooloo, E. Ramos, C. Ries, A. Riffeser, V. Rosenbush, P. Rousselot, E. L. Ryan, P. Santos-Sanz, D. G. Schleicher, M. Schmidt, R. Schulz, A. K. Sen, A. Somero, A. Sota, A. Stinson, J. M. Sunshine, A. Thompson, G. P. Tozzi, C. Tubiana, G. L. Villanueva, X. Wang, D. H. Wooden, M. Yagi, B. Yang, B. Zaprudin, T. J. Zegmott, Philosophical Transactions of the Royal Society A, 375, 2097, (2017).*

VI Evidence of sub-surface energy storage in comet 67P from the outburst of 2016 July 03, *J. Agarwal, V. Della Corte, P. D. Feldman, B. Geiger, S. Merouane, I. Bertini, D. Bodewits, S. Fornasier, E. Grün, P. Hasselmann, M. Hilchenbach, S. Höfner, S. Ivanovski, L. Kolokolova, M. Pajola, A. Rotundi, H. Sierks, A. J. Steffl, N. Thomas, M. F. A'Hearn, C. Barbieri, M. A. Barucci, J. -L. Bertaux, S. Boudreault, G. Cremonese, V. Da Deppo, B. Davidsson, S. Debei, M. De Cecco, J. F. Deller, L. M. Feaga, H. Fischer, M. Fulle, A. Gicquel, O. Groussin, C. Güttler, P. J. Gutiérrez, M. Hofmann, K. Hornung, S. F. Hviid, W. -H. Ip, L. Jorda, H. U. Keller, J. Kissel, J. Knollenberg, A. Koch, D. Koschny, J. -R. Kramm, E. Kührt, M. Küppers, P. L. Lamy, Y. Langevin, L. M. Lara, M. Lazzarin, Z. -Y. Lin, J. J. Lopez Moreno, S. C. Lowry, F. Marzari, S. Mottola, G. Naletto, N. Oklay, J. Wm. Parker, R. Rodrigo, J. Rynö, X. Shi, O. Stenzel, C. Tubiana, J. -B. Vincent, H. A. Weaver, B. Zaprudin, MNRAS, 469, S606-S625, (2017).*

List of abbreviations

CLT - Central Limit Theorem.
COSIMA - COmetary Secondary Ion Mass Analyzer, a scientific instrument which measures cometary dust onboard Rosetta.
COSISCOPE - imaging microscope, an integral part of the COSIMA instrument.
ESA - European Space Agency.
IDPs - Interplanetary Dust Particles, submillimeter-sized particles of the interplanetary space of the Solar System.
MCMC - Markov Chain Monte Carlo, a type of random walk sampling algorithm used in data analysis.
NASA - National Aeronautics and Space Administration, an agency of the United States federal government.
NavCam - Navigation Camera, an optical navigation system instrument of the Rosetta spacecraft.
NOT - Nordic Optical Telescope, a 2.5m optical Ritchey-Chretién telescope located at La Palma, Spain.
OSIRIS - Optical, Spectroscopic, and Infrared Remote Imaging System, the camera system onboard Rosetta.
PSF - Point Spread Function, an instrument function of an optical imaging system.
S/N ratio - Signal to Noise ratio.
TOF-SIMS - Time-Of-Flight Secondary Ion Mass Spectroscopy, a chemical analysis technique.
67P/C-G - the comet 67P/Churyumov-Gerasimenko.

Chapter 1

Introduction

Comets have always fascinated mankind. Since the dawn of history, comets were observed and their appearance was attributed to all kind of interpretations, while the true nature of comets remained a great mystery. Prehistorical cave paintings representing comets and other celestial bodies have been discovered around the world, indicating a sustained interest of ancient people towards cometary apparitions. Usually, comets were believed to be a bad omen or messengers of a forthcoming menace for the whole mankind. In 1456, Pope Callixtus III named Halley's Comet to be "an instrument of the Devil".

There might be a grain of truth in this, since an average-sized comet, speeding from outer space with average cosmic velocities of 40 km/s, could, on impact, inflict widespread destruction of Earth's ecosystem with mass extinctions and could completely wipe out humankind. Fortunately, the impact rate with comets is rather low, approximately one in 33 to 64 million years on average (Sekanina & Yeomans 1984). In contrast, small cometary debris constantly strikes our planet in the form of almost invisible micrometeorites and annual meteor showers, which present spectacular shows in the night sky. The most famous one is the yearly Perseid meteor shower, observed in the middle of August and assumed to originate from the tail of the comet 109P/Swift-Tuttle (Jenniskens 2006).

However, there is the other side of the coin. According to some estimates (Mayo Greenberg & Mendoza-Gómez 1992), abiotic complex organic compounds found in the cometary material might have seeded the primordial Earth with many components needed for the emergence of life. Those organic compounds have also been found in the smallest fragments

of cometary dust (Fray et al. 2016), which are ejected from the comets during the activity periods and which may later find their way into every corner of the Solar System, including the Earth. The smallest IDPs (Interplanetary Dust Particles) of cometary origins can decelerate themselves in the Earth's atmosphere with relatively little entry heating (Szydlik & Flynn 1992), preserving some of the original organic compounds. Descending onto the Earth's surface and the oceanic floor, those organics could aid the emergence of the first living creatures. Comets are also the most pristine objects in the Solar System. Formed on the outskirts of the Solar System and staying far from destructive solar radiation for most of their life, comets preserve the imprints of the Protosolar Nebula and the Solar System formation processes as they were more than 4 billion years ago. From the physical properties, chemical composition and isotopic patterns of cometary material we can, therefore, estimate the conditions in which comets, along with the rest of the Solar System, were formed.

In the last decades, cometary science has advanced to a whole new level. This was possible due to numerous spacecraft missions accomplished by various space agencies, mainly ESA (European Space Agency), NASA(National Aeronautics and Space Administration), ISAS(Institute of Space and Astronautical Science) and the Soviet Space Program. At first, there were flyby missions like ICE, Sagitaki, Giotto, which flew through the coma of comet 1P/Halley and took close-up images and other snapshot measurements of the comet. Later, a notable sample return mission, Stardust, was performed by NASA. At last, the new benchmark for cometary space missions was set by the long term follow-on mission, Rosetta, designed and performed by ESA.

Cometary missions have provided us with a huge amount of new data and precious information, but they also have shortcomings. The main limitation is that not all of the comets are reachable by spacecraft missions. Potential target comets need to have an orbit that is predictable well in advance, during the design stage of the mission. Also, the eccentricity of the orbit, and hence the velocity of the comet in the inner Solar System, should be moderate in order for the spacecraft to be able to intercept it. Those requirements exclude all the long-period and aperiodic comets with highly elliptic or hyperbolic orbits - practically all the Oort cloud objects (Huebner 1990). Beautiful comets like C/1956 R1 (Arend-Roland) would

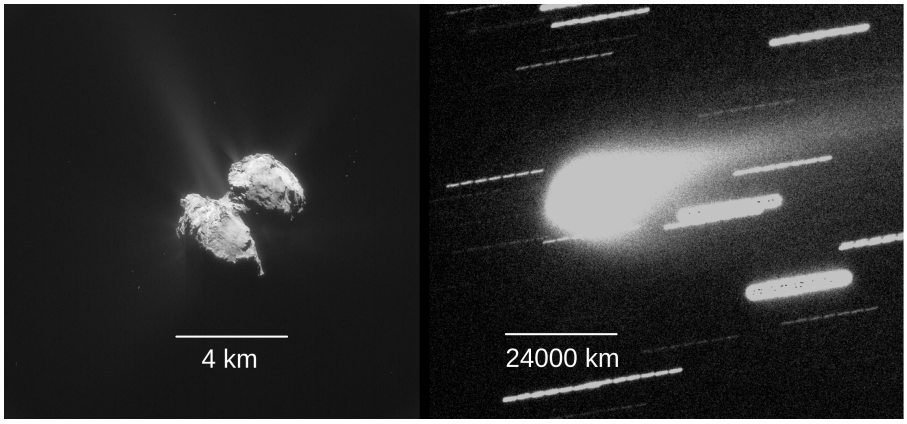

Figure 1.1: The spatial scales of the cometary comae. The image of the nucleus of comet 67P/Churyumov-Gerasimenko observed with the NavCam camera onboard Rosetta spacecraft (Image by ESA) is compared to the ground-based observations with the Nordic Optical Telescope.

never be achievable for spacecraft investigations - at least with the current level of technology. This is a serious drawback that introduces a selection bias to cometary science. The second limitation is economics. Spacecraft missions are far too expensive and time consuming to be mass-produced. We therefore cannot expect a statistically significant amount of comets to be investigated *in-situ*, limiting ourselves to only few cases like comets 1P/Halley, 81P/Wild, 9P/Tempel, 67P/C-G and some others visited by spacecraft within the last three decades.

In contrast, ground-based observations do not have such limitations and any class of comets can be observed. Hence, the whole ensemble of comets can be investigated and solid statistical conclusions can be drawn. Remote observations can cover the vast scales of the whole coma whereas spacecraft instruments always provide local measurements (see Figure 1.1). There are, however, some problems concerning the interpretation of ground-based observations. Comets are usually far away, therefore spatial resolution and S/N ratio can be rather limited. Cometary comae are optically thin, which implies that all the three-dimensional features are projected on a two-dimensional image of the sky. This can lead to misleading results

if two physically unrelated features overlap on this projection. Among other problems there are the unknown optical properties of the cometary dust. This makes several parameters, for example the dust size distribution, number density, albedo and refractive index impossible to estimate independently without introducing models or strong assumptions. Only by combining ground-based observations and *in-situ* data obtained by space missions, can we have an independent reference for some of the critical parameters. Once the clear connections are established and hypotheses tested, we can transfer our knowledge onto the comets where no spacecraft mission is feasible, providing us with a better understanding of comets in general.

This thesis will cut through the dusty coma of 67P/C-G - the target comet of the Rosetta mission. In the research publications presented here, the ground-based observations with the Nordic Optical Telescope were combined with the *in-situ* results of the Rosetta mission. This bridges the gap of spatial scales: from the whole size of the observable coma, reaching up to 10^5 kilometers, to the microscopic size of individual dust grains obtained with the COSIMA instrument. The evolution of a global coma morphology of 67P/C-G was monitored in paper IV and successfully connected with the observations made by Rosetta instruments, explaining seasonal changes observed for several apparitions.

As usual with any kind of research, more questions arose than answers obtained. The most evident is the discrepancy between the *in-situ* data of dust size distribution estimated in paper III with the size distributions required to explain the column brightness of scattered light observed from the ground (Fink & Rinaldi 2015). The scattering efficiency would require the presence of a small micrometer-sized dust which was not detected in sufficient quantities in the COSIMA samples. This would imply either heavy bias in the size distribution of dust collected by COSIMA, or the fragmentation of the dust occurring in a coma above Rosetta's orbit. This, along with other questions, sets the direction of further research. Hopefully, the experience of connecting Rosetta's data to ground-based observations will later help us to solve similar problems on other comets, where the same observed phenomena could lead us to the similar conclusions even without a hint from the spacecraft. This is extremely important for the long-period or aperiodic comets which cannot be reached by spacecraft.

Chapter 2

History of cometary observations and space missions

Comets might have been sighted already in the prehistorian times. One of the oldest representations is located in the state of Bahia, Brazil, dating back "at least ten thousand years ago" (Mour 2009). Although many cave paintings have been assumed to represent comets, their simplified style makes precise interpretation difficult. Also, the exact dating of such art can be challenging. The most famous cave painting of a comet, a tourist attraction, is located in the Chaco Canyon, New Mexico (see Figure 2.1), and presumably dates back to 1066 AD. The sky, eternal and unaltered, at least on the scale of a human lifespan, suddenly presents a new odd looking fuzzy star with a tail, unlike anything that has previously been seen on the Earth. The influence of comets on the minds of ancient humans could be an interesting topic for the paleopsychological research on its own.

Whether feared, admired or ignored, the true nature of comets was not known until modern days. An idea commonly accepted in the Middle Ages in Europe came from Aristotle, who claimed that "comets were nothing but a terrestrial vapor set on fire in the lower highs of the atmosphere located well below the Moon" (Van Nouhuys 1998). This view dominated the minds of European scholars until the age of the Renaissance, when the Danish astronomer Tycho Brahe measured the parallax and calculated the distance to the comet that appeared in the sky in 1577. His results indicated that the comet was located much further than the Moon and is therefore a true

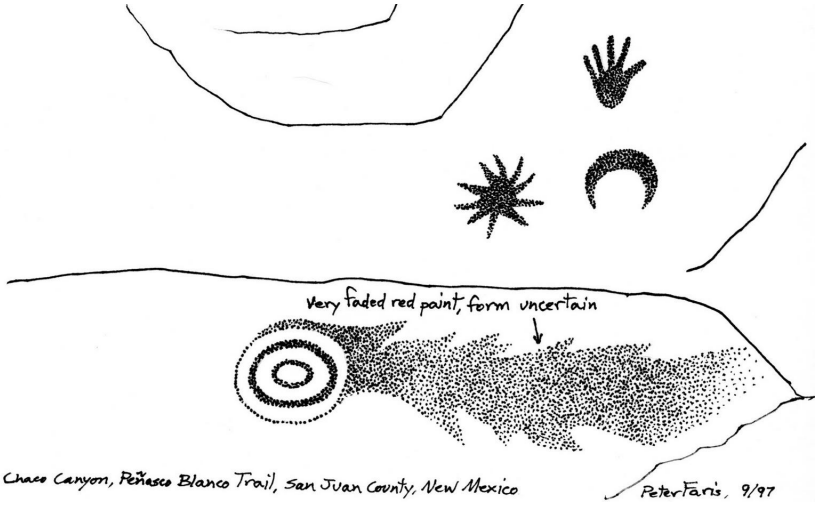

Figure 2.1: A field sketch of a cave painting in Chaco Canyon which represents a comet along with other celestial bodies (Peter Faris, 1997).

celestial body, not an atmospheric phenomenon. At this point, the modern observational cometary science had begun. Halley and Newton had calculated the orbits of several comets, showing them to revolve around the Sun on their elliptic orbits, just like the planets of the Solar System. The high eccentricity of their orbits made the comets penetrate the "celestial spheres" of Solar System planets, postulated to be solid by Aristotle. This discovery played a significant role in the establishment of the Heliocentric model of the Universe (Van Nouhuys 1998). However, it took some time before the atmospheric theory was completely rejected by scholars and the Aristotelian teachings, based on no observational argument in support of his opinion, were declared obsolete.

The nature of comets as celestial bodies has also helped to understand their periodic reappearings. The new apparitions of comet 1P/Halley were predicted by Edmond Halley to take place in the years 1759, 1835 and 1910. The latest of those apparitions was the first time the comet was photographed and the spectroscopic analysis was performed, discovering many unexpected chemical compounds, like cyanide (Stoyan & Dunlop 2015).

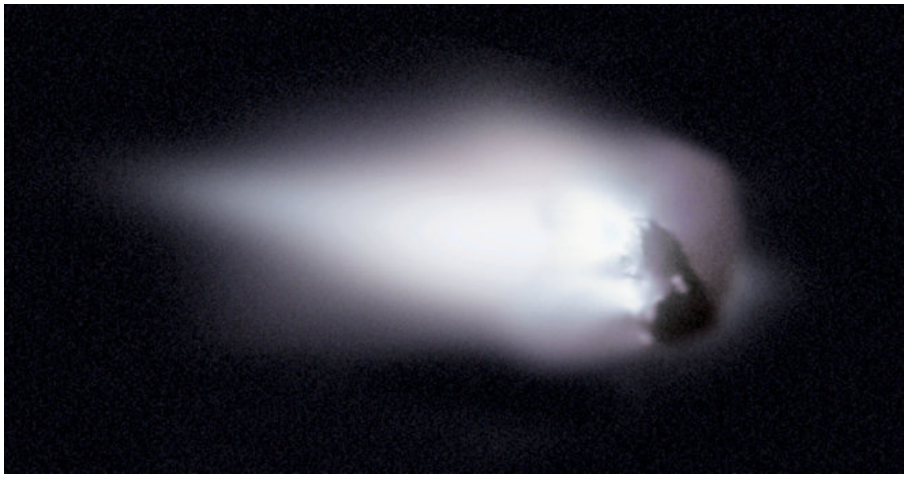

Figure 2.2: Composite image of the nucleus of comet 1P/Halley observed with the Giotto spacecraft in March 1986 from a distance of 600km (ESA. Courtesy of MPAe, Lindau).

By the middle of the 20th century, several theories attempted to explain the physical characteristics of the cometary nuclei. The dominating one was the "gravel bank" model, sometimes also referred to as the "sand bank" model. Within this theory, the nuclei of comets were described as a stack of rocky boulders and pebbles covered with ice and held together by a gravitational attraction. This theory, however, failed to explain the survival of comets with highly elliptical orbits during their perihelia (Fernandez 2006). In 1950, Fred Lawrence Whipple proposed a new model which described the cometary nucleus as a dirty snowball, rather than an icy pile of rocks (Whipple 1950). This theory later evolved into a slightly deviating modern "icy dirtball" concept, proposed by Keller et al. (1986) after the first spacecraft observations of comet 1P/Halley.

A qualitatively new age of cometary exploration started on September 11, 1985, when the International Comet Explorer (ICE) space probe provided the first flyby data from comet 21P/Giacobini-Zinner. A fleet of six spacecraft was also sent to chase the famous comet 1P/Halley, reappearing in the sky in 1986 (see Figure 2.2). The coma density was then measured

for the first time *in situ*, showing a staggeringly low vacuum-like result of $\sim 10^7$ molecules/cm^3 (Krankowsky et al. 1986).

Later, the Stardust space mission was launched by NASA. Its aim was to approach comet 81P/Wild and to return samples of cometary dust particles on Earth. In January 2004, the spacecraft flew through the coma of its target comet and captured sample particles in an aerogel collector. The particles were returned to Earth in 2006 and scientists were able to use terrestrial instrumentation to recover precious information from the samples. The most interesting results were the discovery of complex organic molecules, including glycine (Brownlee 2014).

Up to this day, cometary research has culminated with the Rosetta mission, the flagship of the ESA scientific fleet. Rosetta has inherited most of its scientific tasks from the previously canceled CRAF (Comet Rendezvous Asteroid Flyby) mission by NASA which intended to follow its target comet for a prolonged period of time. Rosetta accomplished that and, in addition, deployed a lander module, Philae, onto the comet's surface, setting the new benchmark for cometary science in the future.

Chapter 3

Comet 67P/Churyumov-Gerasimenko

The target of this research is comet 67P/Churyumov-Gerasimenko (67P/C-G). It appears to be a Kuiper Belt object which has slowly formed in the cold protosolar disc 4.6 Gyr ago and has undergone very little alteration from those times (Davidsson et al. 2016). The nucleus of 67P/C-G has a mass of $9.982 \pm 0.003 \times 10^{12}$ kg and a bilobe structure (see Figure 3.1), with large lobe dimensions of approximately $4.1 \times 3.3 \times 1.8$ km and small lobe dimensions of $2.6 \times 2.3 \times 1.8$ km. The bulk mass of the nucleus consists mostly of silicate material, organics and ices, and has a high porosity of 72-74 per cent. This explains the rather low bulk density of 533 ± 6 kg/m^3, approximatively half of the density of water (Pätzold et al. 2016). A large-scale layering of the nucleus lobes along with the erosion features point out that comet 67P/C-G is likely to be a contact binary object. This would imply that the two lobes, similar but separate objects in the past, have undergone an extremely soft collision at a very low velocity, presumably in the protoplanetary disk during Solar System formation (Rickman et al. 2015).

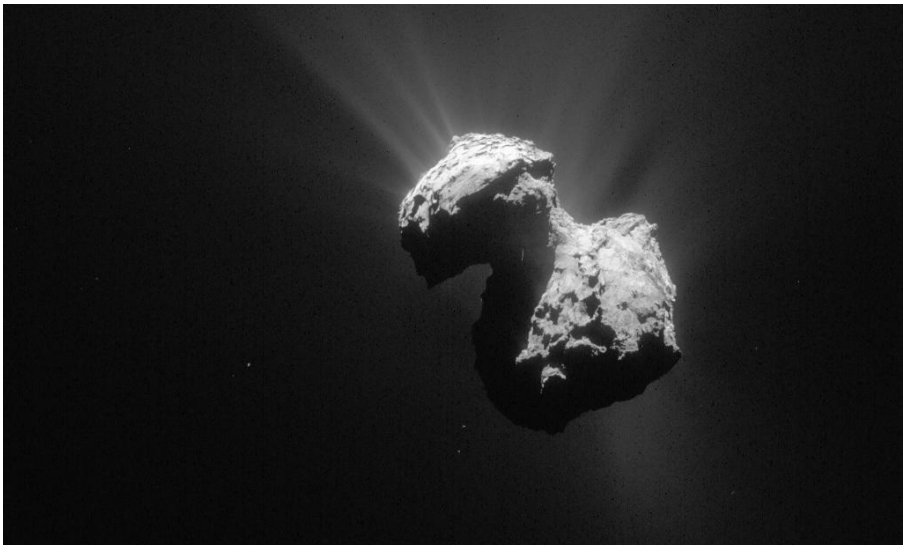

Figure 3.1: Image of the nucleus of comet 67P/C-G obtained with the NavCam instrument onboard Rosetta on the 7th of July 2015 (ESA/Rosetta/NavCam).

The comet has been observed during the last eight apparitions: in 1969 (discovery moment), 1976, 1982, 1989, 1996, 2002, 2009 and 2015. 67P/C-G is now a short period Jupiter-family comet, which means that its orbit is heavily affected by Jupiter's gravitational influence. The comet has an orbital period of 6.45 years and quite a short rotational period of 12.76 hours. The rotation period has decreased after the previous apparitions and probably continues to change. This may happen due to activity induced torque, proposed by Mottola et al. (2014).

The orbital history of 67P/C-G is quite complicated and not well defined. The comet was formed in the Kuiper Belt and later brought into the interior of the Solar System by a series of close encounters with Jupiter. It is estimated that before 1840, the perihelion distance of 67P/C-G was around 4 AU, implying very little or no activity up to those times. However, it has been shown that the orbit of the comet was chaotic before the close encounter with Jupiter in 1923 (Maquet 2015), meaning that tracing the orbital evolution into the deep past is practically impossible.

The last close encounter with Jupiter happened on February 4, 1959, when the perihelion distance was drastically reduced from 2.7 AU before the encounter to 1.3 AU after the encounter (Maquet 2015). Comet 67P/C-G has been on a low perihelion orbit for less than 60 years. It is speculated that during this time, the comet has lost a surface layer of up to several hundred meters (Sierks et al. 2015), exposing fresh pristine material untouched for 4.5 billion years - practically since the formation of the Solar System. This made comet 67P/C-G the perfect candidate for the scientific purposes of the Rosetta mission.

Chapter 4

The Rosetta mission and the COSIMA instrument

The Rosetta mission has a completely new philosophy compared to the cometary space missions of the past, all of which were flyby missions like Giotto or sample return missions like Stardust. Mission designers have decided not to take cometary samples to a terrestrial laboratory, but rather to send the laboratory to the comet. This approach has the great advantage of providing a continuous stream of *in situ* data for a prolonged period of time, allowing us to study the temporal evolution of the physical properties of the comet's nucleus and coma along its orbit and throughout the most active phase at the perihelion. Rosetta's orbiter module performed scientific tasks at close proximity of comet 67P/C-G for over two years, while the lander module, Philae, achieved the first successful landing on a cometary surface - although with some problems partly compromising its scientific activity (Biele et al. 2015).

The Rosetta orbiter module had twelve scientific instruments on board (see Figure 4.1), including several visible, IR and UV imagers and spectrographs: NavCam(Navigation Camera), OSIRIS (Optical, Spectroscopic, and Infrared Remote Imaging System, the camera system onboard Rosetta), ALICE and VIRTIS (Visible and InfraRed Thermal Imaging Spectrometer); a microwave instrument MIRO (Microwave Instrument for the Rosetta Orbiter) and radio instruments CONSERT (COmet Nucleus Sounding Experiment by Radiowave Transmission) and RSI(Radio Science Investigation). The plasma environment was measured by RPC (Rosetta Plasma Consortium) and the gaseous coma by ROSINA (Rosetta Orbiter Spectrometer for

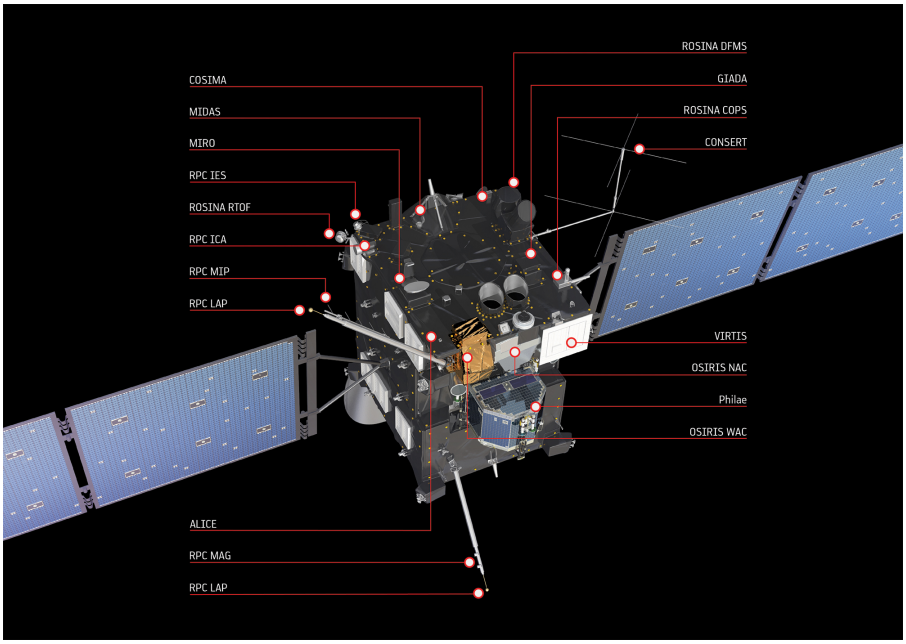

Figure 4.1: The instruments of the Rosetta mission located on the spacecraft (ESA/ATG medialab).

Ion and Neutral Analysis). The dust of comet 67P/C-G was monitored by several complementary instruments: MIDAS (Micro-Imaging Dust Analysis System), an electron microscope concentrating on the smallest observable grains, GIADA (Grain Impact Analyser and Dust Accumulator), an instrument measuring the mass, velocity and optical cross-section of captured grains and COSIMA (COmetary Secondary Ion Mass Analyser), a versatile instrument which combines a dust collector, an optical microscope and a secondary ion time-of-flight mass spectrometer. The data provided by the COSIMA instrument were intensively used in this work to analyze the physical and statistical properties of cometary dust particles.

Rosetta's journey to comet 67P/C-G took more than ten years, during which time it performed several gravity maneuvers around Earth and Mars, and close flybys of asteroids Stein and Lutetia. Rosetta's rendezvous with its final target took place in August 2014, right after the activity of the

comet started to rise. Rosetta followed the comet throughout its perihelion, capturing the peak activity (Vincent et al. 2016), single massive outbursts (Grün et al. 2016), as well as long term degradation of surface material (Pajola et al. 2017). Some of the most important results were rather unexpected, such as the presence of molecular oxygen (Bieler et al. 2015a) and the high D/H isotopic ratio (Altwegg et al. 2015). New results for the Solar System formation and astrobiological studies were also obtained, as the TOF-SIMS spectra of the cometary dust have indicated the high abundance of extremely large refractory organic molecules, more complex than anything ever detected in comets before (Fray et al. 2016). Rosetta has had a large impact in the media, where most of the public interest was captured by the amazing images obtained with the OSIRIS and the NavCam visual cameras.

One of the three dust instruments onboard the Rosetta spacecraft is COSIMA. The main functions of the instrument are the TOF-SIMS analysis of the cometary dust chemical composition and the optical analysis of the grains with the built-in microscope called COSISCOPE (Kissel et al. 2007). While the former technique can help us to understand the chemistry of the cometary grains and isotopic abundances of the key elements, the latter can provide us with valuable information about the statistical properties of the dust, for example particle size distribution, albedo, morphology, porosity and many other parameters. Based on the observations with COSISCOPE, even the tensile strength of the dust particles can be estimated (Hornung et al. 2016).

A layout of the COSIMA instrument is presented in Figure 4.2. COSIMA consists of three main functional modules: the target manipulator unit, the optical microscope (COSISCOPE) and the secondary ion time-of-flight mass spectrometer. The dust is collected by exposing silver or gold substrate plates into the space inside of a dusty coma. The cometary grains, directed by a funnel, get attached to those substrates with very low impact velocities, usually of order of a few meters per second (Hilchenbach et al. 2016). After the exposure, a robotic arm moves the substrates to either a storage room, a chemical station where the substrates can be heated, or into the TOF-SIMS measurement position.

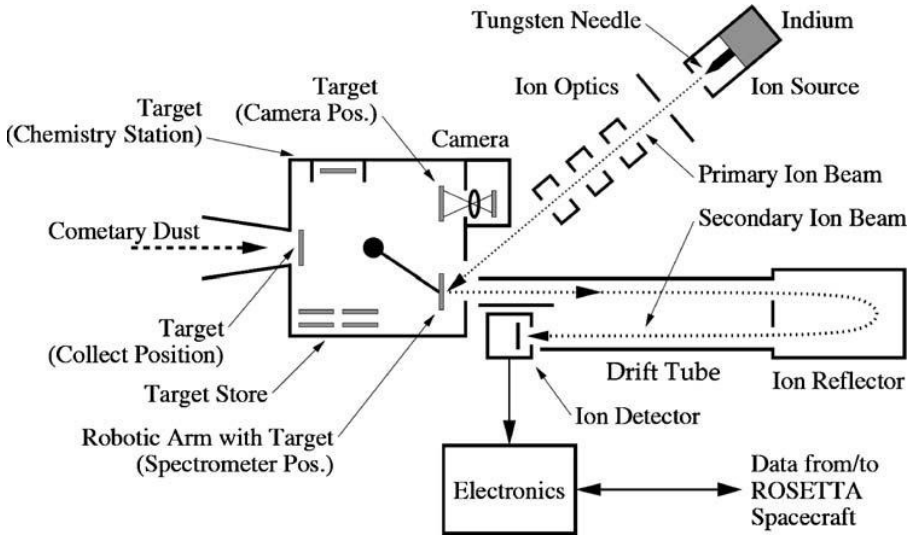

Figure 4.2: Principial layout of the COSIMA instrument (Kissel et al. 2007).

The mass spectra of the grains are obtained via the TOF-SIMS technique. The instrument operates by shooting the dust grains with a pulsed In^+ beam, which produces secondary ionization in the target material. The produced secondary ions are picked up by an electric field and fed into the ion deflection arm of the instrument. The mass of the secondary ions can be calculated from their time of flight through the drift tube and the deflector. From the mass spectra, the abundances of the chemical elements and molecular fragments can be estimated. COSIMA has a native resolution of 2000 at mass 100 amu (Kissel et al. 2007), which allows to separate organic ions from their mineral counterparts at the same integer mass. For example, the $C_2H_4{}^+$ ion can be easily resolved from the $^{26}Mg^+$ ion. However, some ion peaks with a small mass separation are overlapping in the spectra, and for example the $^{57}Fe^+$ peak cannot be resolved from the $^{56}FeH^+$ peak. The resolving capability decreases with a decreasing S/N ratio which is usually quite low for many scientifically interesting cometary compounds (Hilchenbach et al. 2016). More detailed information about the statistical analysis of the COSIMA instrument, along with the newly developed way of analyzing low signal-to-noise TOF-SIMS data are presented in paper I.

Chapter 5

Analysis tools and Bayesian statistics

As the sharpening of woodcutting tools is an essential part of a carpenter's work, is the development of mathematical methods an essential part of astronomical research, even though neither the wood nor the celestial bodies are directly addressed. As measurement techniques, models and conclusions become more and more complicated, the correct interpretation, inference and error analysis become of utmost importance in modern science. The central idea of modern physical sciences is to build a mathematical model of reality that would be able to predict the outcome of the experiment - and to verify this prediction by comparing it with the actual experiment. This always incorporates statistics, as no model parameters are known to infinite precision, nor are the measurements exact. In addition, models themselves are usually approximate.

Concepts of dealing with probabilities or uncertainties have historically been divided into two main branches: the frequentist approach and the Bayesian approach. While the former considers the probability as the relative frequency of a certain outcome in a long series of trials, the latter defines the probability as the 'degree of belief' we put in a current theory (Gelman et al. 2004). While both approaches have their applications in science, the Bayesian interpretation has become the common way of determining statistical inference, mostly due to its flexibility and ease of incorporation in computer simulations. In simple problems, where both approaches are applicable and sufficient to correctly represent the statistics, both should provide the same results. Although Bayesian statistics is a wide scientific

discipline which cannot be fully presented on a few pages, the central ideas of the methods used in this research work are shortly summarized in this chapter.

Bayesian data analysis as a statistical tool plays a central role in this work. Paper I describes a Bayesian peak fitting algorithm developed and used to analyze the COSIMA spectra. In paper II, Bayesian statistics combined with MCMC (Markov Chain Monte Carlo) methods were used to resolve the coma of comet 67P/C-G from its nucleus using data with weak spatial resolution. In paper III, Monte Carlo simulations were used to determine the degree of randomness of the spatial distribution of cometary dust particles on the collector plates of the COSIMA instrument.

In practice, Bayesian data analysis starts with the examination of the error distribution of the instrument or intrinsic physical phenomena behind the measurement, providing the expected statistical noise of the system. In many applications, the Central Limit Theorem (CLT) can be incorporated, reducing the probability distribution of a mean of multiple independent measurements into a Normal distribution:

$$P(\theta|M) \approx N(\mu, \sigma^2) = \frac{1}{\sqrt{2\pi\sigma^2}} e^{\frac{(\mu-x)^2}{2\sigma^2}} \quad , \tag{5.1}$$

where μ is the mean of the distibution and σ is the square root of the variance, the width parameter of a Gaussian curve. This parameter became the standard textbook way of indicating the measurement errors and statistical significance of observations and the common least-square fitting is based on a CLT approximation. For example, the statistical significance of the detections of comet 67P/C-G on the early observations was expressed in sigma parameters, as presented in the supplement tables of paper II. Another example is the famous detection of the Higgs boson with a statistical significance of 5.9σ, as reported by Aad et al. (2012).

If the error distribution of a single measurement is not Gaussian, or the sample size is not large enough to justify the application of the CLT, statistical problems may become complicated with no suitable standard method available. For example, in the analysis of COSIMA spectra presented in

paper I, ion counts at each TOF channel follow a Poisson distribution:

$$P(\lambda, k) = e^{-\lambda}\frac{\lambda^k}{k!} \quad , \tag{5.2}$$

where λ is the mean value of the distribution and k is the number of occurrences of the stochastic event.

The probability of a single datapoint measurement given the prediction of the model is thus $P_i(M_i|\theta) \approx Poisson(M_i|y_i)$. Combining multiple datapoints is done by estimating the joint probability for all mutually independent measurements:

$$P(M|\theta) = \prod_i (P_i(M_i|\theta)) \quad , \tag{5.3}$$

or equivalently

$$log(P(M|\theta)) = \sum_i (log(P_i(M_i|\theta)) \quad . \tag{5.4}$$

The logarithmic representation is used for two reasons. Firstly, the absolute value of $P(M|\theta)$ can be so small that the numerical precision of the computer is not sufficient to describe it. Secondly, the sum is practically much easier to calculate than the product.

A special feature of Bayesian inference is the use of the prior distributions. Although disputed for being subjective, prior distributions are an elegant way to introduce our knowledge of the physical system or correct the observational biases in the statistical model. In fact, a properly assigned prior distribution can have an objective justification, while, for example, choosing $\sum^i (x_i - \bar{x})^2$ as the parameter of minimization introduces a subjective assumption of the statistical properties of the problem (Gelman et al. 2004). Basically, not using prior distributions, as done in frequentist statistics, implies ignorance towards our knowledge of the system.

The prior distributions can be informative or non-informative. While an informative prior distribution describes the previously known information about the system and adjusts the probability accordingly, a non-informative prior distribution does not interfere with the likelihood. In the COSIMA

spectra peak fitting routine, introduced in paper I, a non-informative prior distribution was originally used, as we do not have any reasonable and unbiased estimate for the chemical composition of the target or the peak shape behavior prior to the measurements. In later versions of the routine, more complex hierarchical models were introduced which defined a weakly-informative prior distribution for the shape of the spectral peak measured at the part of the spectra of the highest S/N ratio. Such hierarchical models have been described in detail by Gelman et al. (2004).

In many applications, the likelihood of the model $P(M|\theta)$ is not easy to define analytically and can be estimated only numerically relying on the pseudorandom numbers provided by a computer. The computer simulates the physical processes and provides the final distribution of randomly occurring events. In this way, the occurrence probabilities for every possible outcome can be estimated. These simulations are called Monte Carlo simulations. Such simulations were used in this work in paper III, where the randomness of the spatial distributions of the dust particles collected on the substrates of COSIMA was tested using this method.

The final posterior probability $P(\theta|M)$ can be obtained from the measurement likelihood defined by equation (5.4) combined with the prior probability $P(\theta)$. This is achieved using Bayes' theorem:

$$P(\theta|M) = \frac{P(M|\theta)P(\theta)}{P(M)} \quad . \tag{5.5}$$

Thus far, only the probability for a model $M(\theta)$ with a single defined parameter set θ was considered. However, the aim of the Bayesian fitting procedure is to find a parameter set with the best posterior probability $P(\theta|M)$ among all the possible sets of parameters θ, as well as to constrain an area in the parameter space where this probability is significant. The distribution of the posterior probabilities in this parameter space is called the posterior distribution.

Mapping the posterior distribution analytically is usually not an easy task, and this was the main reason why Bayesian statistics were rarely used in science before advances in computer technology. With the aid of modern computation power and numerical methods, even the posterior distribu-

tions of extremely complex physical models with hundreds of parameters can be calculated (Tamminen et al. 1998).

The most straightforward but inefficient method is simply to calculate the posterior distribution at every point of the parameter space - usually using evenly spaced grids. This is called the brute force method and it is still popular in some simple minimization routines. The problem with this method is that the whole parameter space has to be evenly sampled while the desired posterior distribution may be strongly localized. In multidimensional problems this can be prohibitively expensive in terms of required computation power.

In many applications, a good way to map the posterior distribution is to use MCMC methods. These methods rely on random walk algorithms which, during each step, sample a new point from the parameter space and accept or reject this transition with a probability dependent on the calculated posterior probabilities. According to their definition, Markovian chains imply no memory effect. This means that the transition from the point θ_1 to θ_2 in a random walk algorithm is not affected by θ_0 or any other previously sampled point of the parameter space. However, in some cases, even this requirement is not essential if some approximations of the shape of the posterior distribution can be made, as the performance of the Adaptive Metropolis algorithm indicates (Saksman & Vihola 2008).

Once the posterior distribution is sampled, the maximum posterior probability point can be regarded as the 'best fit' parameter set. The rest of the posterior distribution is used to define confidence intervals - a Bayesian counterpart of traditional error bars. The confidence intervals normally used to represent errors are 68%, 95.4% and 99.7% limits which constrain a subarea of the parameter space that encloses 68%, 95.4% or 99.7% of the total hypervolume of the posterior distribution. Sometimes, the posterior distribution is well approximated by a multivariate normal distribution. In those cases, the confidence intervals mentioned above correspond to the traditional error limits of 1σ, 2σ and 3σ, respectively. An extremely useful feature of the MCMC method is that the number of steps sampled around a certain point of the parameter space is proportional to the value of the posterior distribution at that point. Therefore, the error limits of 68%, 95.4% or 99.7% can be easily estimated by counting 68%, 95.4% or 99.7%

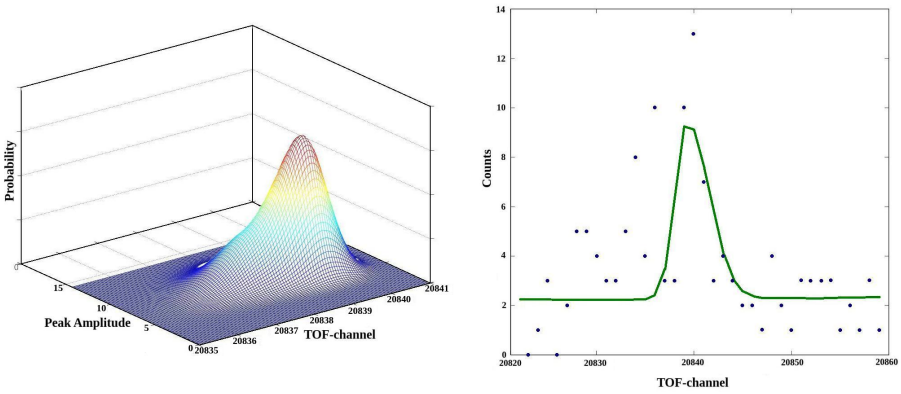

Figure 5.1: Bayesian analysis of a very weak signal ion peak from a COSIMA mass spectrum. On the right, actual data from the instrument is presented with dots, while the best fit peak model is represented by a solid green line. The calculated posterior distribution in the simplest case of a two-dimensional parameter space (peak position vs. peak magnitude) is presented on the left. The z-direction represents a posterior probability expressed in an arbitrary unit.

of the sampled step points of the properly converged MCMC chain.

Paper I of this work describes the implementation of an Adaptive Metropolis MCMC-algorithm to analyze the TOF-SIMS data of the COSIMA instrument. In Figure 5.1, an example of the output of such a fitting routine is presented. On the left, the estimated posterior distribution is shown with a three-dimensional plot. The red and yellow subarea of the plot covers the sampled parameter space that represent the 68% confidence intervals. Noticeably, the posterior distribution can in some cases be very different from the multivariate Gaussian distribution. In such cases, the traditional $\pm 1\sigma$ symmetrical error limits cannot be applied.

Chapter 6

Ground-based observations in support of Rosetta

6.1 Observation techniques

Until the latest decades, the only available observations of comets or any minor celestial bodies were ground-based observations, first performed with bare eyes, later with various optical telescopes equipped with photographic plates. Advances in detector technology have helped us to expand from the visual range to the infrared, UV and radio, as well as enabled spectroscopy and polarimetry. Still, all the observations remained ground-based in those times, which in turn had its own restrictions: limited periods of visibility, large distances to the targets, loss of resolution due to the atmosphere and telluric contamination obscuring cometary features of interest. Only in the latest decades, cometary missions such as ICE, Giotto, Stardust and Rosetta have helped us to surpass those restrictions and get a grip on first-hand *in-situ* data of comets. Through close-up images of cometary nuclei, gas and dust chemical analyses, microscopic studies of dust properties and plasma studies, space missions have hugely advanced our knowledge of cometary physics and chemistry.

However, space missions are very limited by their high cost and the extremely high effort needed for planning and executing them. A mission can deliver information of only one or a few suitable objects. Suitable targets for space missions are also limited by their nature, adding observational bias to cometary science. A target's orbit has to be precisely known well in advance and be suitable for a spacecraft rendezvous. This requirement prac-

tically excludes fast sungrazing comets which descend from the Oort cloud unforeseen and sprint through the inner Solar System in a highly elliptical or hyperbolic orbit. In order to avoid those restrictions and to use data obtained from space missions cost-effectively, we have to connect the data with ground-based observations. After that, we can translate these connections to other comets observed from the ground to correctly interpret the discoveries. For a few objects, such as comet 67P/Chyryumov-Gerasimenko presented in this work, both the spacecraft data and the ground-based observations are available. Therefore, the aim of this work is to establish interconnections between the space mission data obtained by the Rosetta spacecraft and the ground observations performed with the Nordic Optical Telescope (NOT).

6.2 Remote sensing

Remote sensing techniques consist of ground-based, airborne and rocket-borne observations including observations performed with spacecraft located far from the target comet. Many sungrazing comets were observed with the SOHO spacecraft close to their perihelion which, per se, can be destructive to the comet. For instance, comet ISON C/2012 S1 was recently disrupted during perihelion passage, as observed by SOHO (Knight & Battams 2014). Ground-based facilities were unable to observe the event because of the angular proximity to the Sun. Another good example of spaceborne observations is the remote imaging of comet 67P/C-G with the Hubble Space Telescope (Lamy et al. 2006). Such remote space observations also avoid the contamination and wavelength limitations imposed by the Earth's atmosphere. Observations from a distant spacecraft may also be important as they view a comet from a different phase angle, therefore complementing observations obtained from the Earth.

By definition, ground-based observations are observations obtained with ground-based facilities which are mainly optical, IR and radio telescopes. These observations can be divided into two major branches: imaging and spectroscopy. While spectroscopy provides us with vital knowledge of the chemical content of the gaseous coma and allows us to make some constraints for the size distribution of light scattering dust, imaging helps us to resolve any spatial properties of the coma, providing the accurate astro-

metric position of the nucleus, the total brightness (photometry), possible signs of outbursts and the coma morphology.

Imaging provides us with even more information if the use of various filters is incorporated. For example, narrow band filters with a pass wavelength of a specific molecular spectral line can be used to study the spatial distribution of gaseous matter in the coma. Polarizing filters can be used to study the light scattering processes of the dust in a coma (Kolokolova et al. 2016). Sometimes, even the naked eye reveals that the ionic tail of the comet is much bluer than the rest of the coma. To make more precise measurements, broadband filters can be used to study the color and, therefore, spatial variations in the gaseous content, the ionization state and the gas to dust ratio. Color is mostly affected by several gaseous species which produce strong emission lines in the visible spectra. The brightest ones are the CN line around 380 nm and the C_2 lines at the wavelengths of 440 nm and 550 nm. Those lines are mostly responsible for the characteristic purple or the greenish glow of comae.

During the NOT monitoring program presented in papers II and IV, two filters were used: Bessel R and V. This allowed us to obtain bicolor images of the comet (see Figure 6.1). A wide-wavelength response of the R (red) filter covers mostly continuum light that has been scattered by the dust or reflected by the nucleus. In contrast, the V filter (green) covers strong spectral lines of the gaseous content of the coma - mostly the C_2 and NH_2 lines (Arpigny 1965). In paper II, separate photometry was performed to investigate whether the activity of 67P/C-G is similar in those two colors. The resulting differences were insignificant and did not exceed the detection limit (S/N ratio lower than 3). This leads us to the conclusion that the activity was relatively uniform in the gas-to-dust ratio and no significant gas-dominated outbursts took place. The same result is observed if the coma is heavily dominated by dust, and gaseous spectral lines provide little contribution to the color of the coma. Later, Rosetta results confirmed this low gas content hypothesis (Moreno et al. 2016).

The usual way of performing a color analysis is to align and normalize the subsequent V and R observations and then subtract one from the other. The resulting image reveals the color differences and therefore the spatial distribution of the gaseous content compared with the dust, or equivalently,

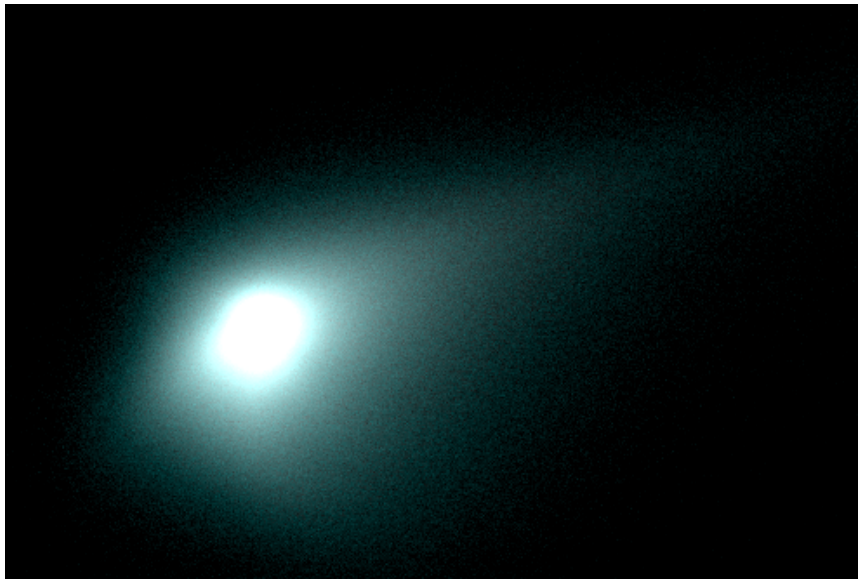

Figure 6.1: A bicolor image of comet 67P/C-G observed with the Nordic Optical Telescope. The normalized V-band brightness is shown in the green and blue channels of the RGB color scale, while the R-band image is shown in the red channel.

the gas-to-dust ratio distribution. On the image, this would be seen as the bright and dark areas in the coma. Such a study was performed in paper IV with the subsequent observations of comet 67P/C-G in both V and R filters. The resulting difference images were flat and no color gradient was detected under visual inspections. This is not a surprising result, as a low gas-to-dust ratio was expected, based on the previous observations of 67P/C-G (Weiler et al. 2004). For other comets, clear gas distribution gradients have been observed. A good example is the color map of the coma of comet C/2000 WM1 published by Lara et al. (2004).

6.3 Astrometry

The technique of measuring an object's location in the sky is called astrometry. As comets are not stationary objects, the position of the target in the sky at any given time has to be predicted. Using modern celestial mechanics, the position can be calculated to high precision, once orbital parameters are known. To do that, we have to track the comet's movement and obtain a sequence of celestial coordinates describing the location of the comet at each time point it was observed.

The usual way of determining the sky coordinates of a celestial body is to compare the location of the target on the observed image with the locations of the known calibration stars (see Figure 6.2). Before measuring the location of the target, the observed images have to be astrometrically calibrated. This means that the conversion from the pixel coordinates of the image to the stellar coordinates on the sky has to be evaluated. The transformation should take into account field distortion caused by the projection effect of the celestial sphere on the imaging plane, in addition to possible distortions caused by the imaging system. A common method normally used in astronomical observations is linear transformation combined with gnomonic projection. This method is described in detail by Calabretta & Greisen (2002).

To derive the astrometric transformation parameters, a good astronomical catalog is essential. In our work, we mostly used USNO-A2 [1], UCAC4[2], GSC[3] and 2MASS[4] catalogs, depending on the field of view. The pixel positions of the calibration stars are presented as the function of their celestial coordinates, and a fitting routine is used to estimate conversion parameters. After that, any pixel coordinates on the image can be easily converted to sky coordinates. The pixel coordinates of the cometary nucleus are measured on the image with subpixel precision. In this work, the optimization algorithms contained in the IRAF (Image Reduction and Analysis Facility) distribution packages (Tody 1986) were used. The error estimate for the astrometric position shall include a standard deviation of the conversion

[1] Catalog of Astrometric Standards of the U.S. Naval Observatory.
[2] Fourth U.S. Naval Observatory CCD Astrograph Catalog.
[3] Guide Star Catalog of the Hubble Space Telescope.
[4] Two Micron All Sky Survey catalogue.

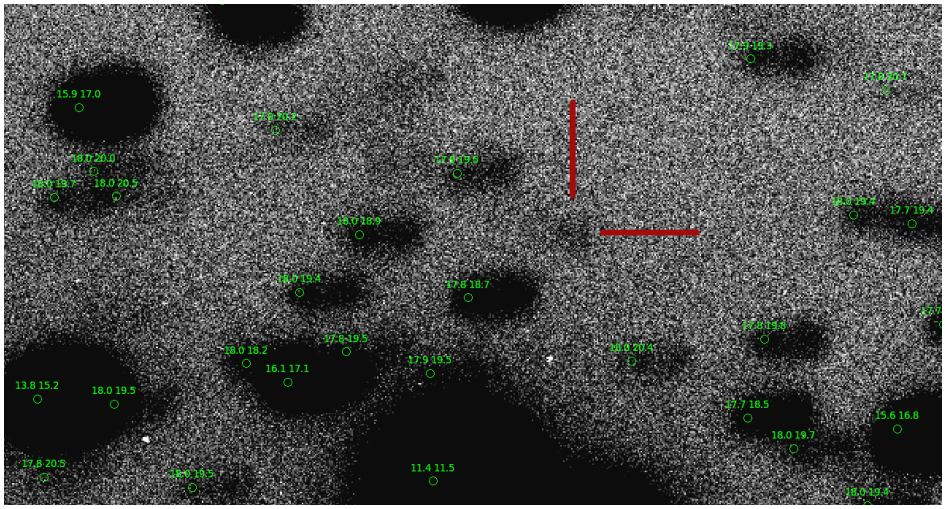

Figure 6.2: One of the first observations of comet 67P/C-G during the 2013-2016 apparition performed with the Nordic Optical Telescope. Locations and magnitudes (**R** and **V**) of the calibration catalog stars are marked on the image. The stars are elongated due to the motion of the comet which has been followed by the telescope.

parameters combined with the error estimates for the measurements of the pixel coordinates of the comet's nucleus.

The astrometry of comet 67P/C-G before Rosetta's rendezvous, presented in this work, was at the time extremely important for the Rosetta mission. Any observed deviation from the comet's location could have meant that the spacecraft should have performed additional maneuvers in order to catch up with the target. Once the comet was reached, the spacecraft telemetry provided its location with even greater precision. An astrometric analysis was performed on the NOT images and the results are presented in Table A.1. These results were in a good agreement with the previous estimates and no additional maneuvers of the spacecraft were needed.

6.4 Photometry

Photometry of comets involves the measurement of the apparent brightness of either the coma, the nucleus or the combination of both. During the inactive phase, when the comet is far away from the Sun and its activity is weak or absent, photometry is similar to the standard procedure normally performed on stars or other point-like sources in astronomy. Such an analysis was performed on a part of the observations presented in paper II, where no significant activity was detected. The resulting lightcurve along with the prediction line made by Snodgrass et al. (2013) is presented in Figure 6.3.

Once comet 67P/C-G became significantly active, the point source approximation no longer held. The diffuse coma can extend from arc seconds to arc minutes from the nucleus, with edges so faint that the real limits are difficult to specify. Photometry of the extended source implies an assumption of the object's brightness profile, usually derived from its physical model. A good example is the assumption of the brightness profile for elliptical galaxies derived from de Vaucouleurs law (de Vaucouleurs 1958), often used in extragalactic astronomy. For cometary comae, no such approximation can be made. Rapidly changing insolation and activity rates imply that the coma is not in a steady state. Additional random factors include discrete eruptions, jets, the irregular shape of the nucleus and the uneven spatial distribution of the volatile compounds on the surface. All of those phenomena were observed on comet 67P/C-G during the Rosetta mission (Jones et al. 2017), which resulted in the peculiar morphology of the coma of 67P/C-G, described in paper IV.

With a large extended coma, only aperture photometry can be performed. The size of the aperture is usually chosen to cover a specific area on the plane of the sky projected to the distance of the object. For example, Boehnhardt et al. (2016) presents the photometry of comet 67P/C-G during its active phase with several apertures, covering the projected distances of 5000 km, 10000 km, 15000 km and 20000 km from the nucleus. This approach compensates for the variations in the spatial scale of the images, caused by varying distance. By examining the sudden temporal changes of the lightcurve of each aperture after an outburst, some estimates can be drawn for the dust particle propagation speed, as the increase in the

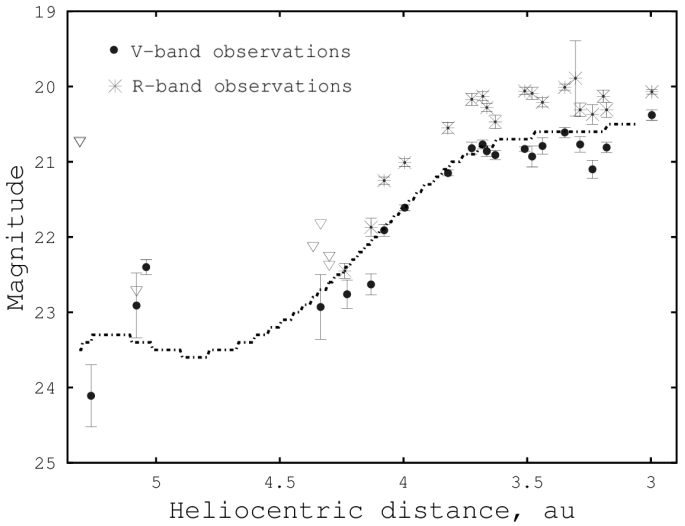

Figure 6.3: Lightcurve of comet 67P/C-G before the Solar conjunction, published in paper II. The dashed line represents the predictions made by Snodgrass et al. (2013), shifted down by 2 magnitudes to match the response of the filters used. Triangles represent the 3σ upper limits for the brightness of the comet for those observations where comet was not detected.

brightness will first appear in the smallest aperture, with larger apertures sequentially following along with the propagation of dust and gas in the coma.

A special situation lies between the two limiting cases of a completely inactive and a fully active coma. When activity has started, the surface brightness profile of the target cannot be approximated as a point source. The brightness of the nucleus and the brightness of the coma, in this case, are comparable. However, the evolution of the brightness of the nucleus can be predicted theoretically from the heliocentric distance Δ and the distance to the observer r using the following formula (Huebner 1990):

$$B \propto r^{-2}\Delta^{-2} \quad . \tag{6.1}$$

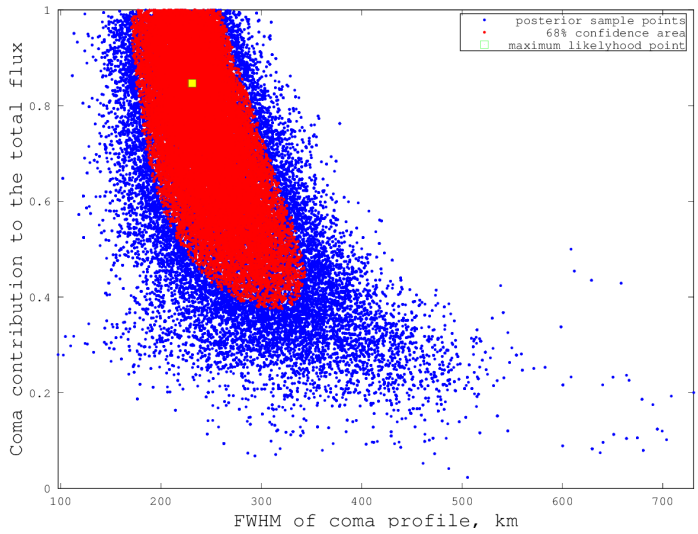

Figure 6.4: A Bayesian fit describing the posterior probability distribution of the coma contribution to the total brightness of the comet and the spatial size of the coma (FWHM) in the observations on the 21st of August, 2014, as presented in paper II. The yellow square indicates the best-fit point while the red area covers the 68% area of the posterior distribution.

This relation does not take into account many phenomena that could affect brightness, such as rotational modulation and an irregularly shaped nucleus, along with a changing phase angle and variations in surface albedo. Therefore, a way to decouple the coma brightness from the nucleus is proposed in paper II.

The presented method relies on the modeling of the observed brightness profile as the sum of the profile of the nucleus, represented by Dirac's delta function convolved with the PSF (Point Spread Function of the telescope measured from the star profiles on the image), and the extended source profile of the coma convolved with the PSF. The model has three free parameters: the flux contribution of the nucleus $B_{nucleus}$, the flux contribution of the coma B_{coma} and the parameterized spatial size of the coma model

$M(R)$.

$$B_{total}(R) = PSF * (B_{nucleus} \cdot \delta(R) + B_{coma} \cdot M(R)) \quad , \qquad (6.2)$$

where R is the projected distance from the nucleus and $M(R)$ is the shape model for the brightness profile. In paper II of this work, an exponential profile is assumed for the brightness profile of the coma. Although the coma equilibrium assumption required to justify such a profile is not always solid, in our case, within the given signal-to-noise ratio, any plausible coma model would not cause major changes in the results. The main goal is to estimate how much of the total brightness appears to originate from the extended source. In most of the pre-conjunction observations presented in paper II, the S/N ratio was not sufficient to perform such an analysis, although for some nights, estimates were derived. Figure 6.4 presents an example, in which the brightness of the coma of 67P/C-G was estimated to comprise between 40% to almost 100% of the total brightness and the size of the coma was constrained to be between 180 km and 350 km in FWHM.

6.5 Coma morphology

The morphology of a coma provides us with valuable information that cannot be derived from the photometry or spectral analysis alone. The spatial distribution of a comet's activity across its nucleus, the velocities of the ejected material and many other effects of interest can be derived by studying the coma morphology. Major outbursts and other sudden temporal activity variations leave long-standing traces in the morphological structure of the coma and can be, therefore, traced back and characterized.

The most commonly observed morphological structures are jets - long narrow structures produced by collimated outflows of gas and dust from the nucleus. Cometary jets are usually curved on large scales, due to Solar wind interaction and radiation pressure, or on smaller scales, due to the rotation of the nucleus and hence the rotation of the source of the jet on the surface. A more diffuse structure with a large opening angle is normally referred to as a fan. The definitions are not exact for those two cases and the terminology often causes confusion. If the active spot on the nucleus is producing ejecta only for a short period of time, the resulting localized cloud of material propagating outwards is called a plume. Eventually, all

the gas and the small dust particles get deflected and form the tail of a comet pointing in the direction opposite to the Sun.

The correct interpretation of the images of cometary comae is far from intuitive. A coma, as it appears to the observer, does not resemble any object that the human eye is used to see in the terrestrial life. Even a thin cloud, mist or smoke are usually optically too thick to make a comparison. The measured gas density of the coma of comet 67P/C-G appeared to be only 10^4 - 10^8 molecules per cubic centimeter (Bieler et al. 2015b), which is comparable to a high vacuum achieved in a laboratory. The size of comae can reach up to 10^4- 10^6 kilometers. Starting from the very proximity of the nucleus, the coma is optically thin and the brightness we observe is just a column of scattered light integrated along the line of sight. This introduces all kinds of projection effects that may lead to misinterpretations. Physically unrelated morphological features can be visually connected and appear like a single structure. A good example can be the 'split tail' of comet 67P/C-G observed during several apparitions (Agarwal et al. 2010). The trail (large cometary debris which stays roughly on the same orbit) and the tail of the comet are brought together by a projection onto the imaging plane, but are completely separate in physical space.

As recovering the coma structure from the observed image is not a straightforward task, a better way is to build a physically plausible three-dimensional model and then integrate it along the line of sight to reproduce the two-dimensional observations. This can be achieved, for example, by utilizing finite element methods, where the three-dimensional array of values represents the coma density distribution in a physical space. The easiest way is to choose a 'z' direction parallel to the axis of the nucleus rotation, and to put the 'x' axis on a plane defined by the 'z' axis and the apparent direction of the Sun. To constrain the parameters of the model, a Monte Carlo technique can be used: for each randomly modified set of parameters, such as locations of the high activity spots on the nucleus, the model is reconstructed and its estimated column brightness along the line of sight is compared with the actual observations. One example of such modeling is presented in paper IV, where the excessive activity of the southern regions of the nucleus is assumed to produce a conical structure in the coma of 67P/C-G due to the rapid rotation of the nucleus around its axis. The projection of this model is straightforward to calculate using basic geome-

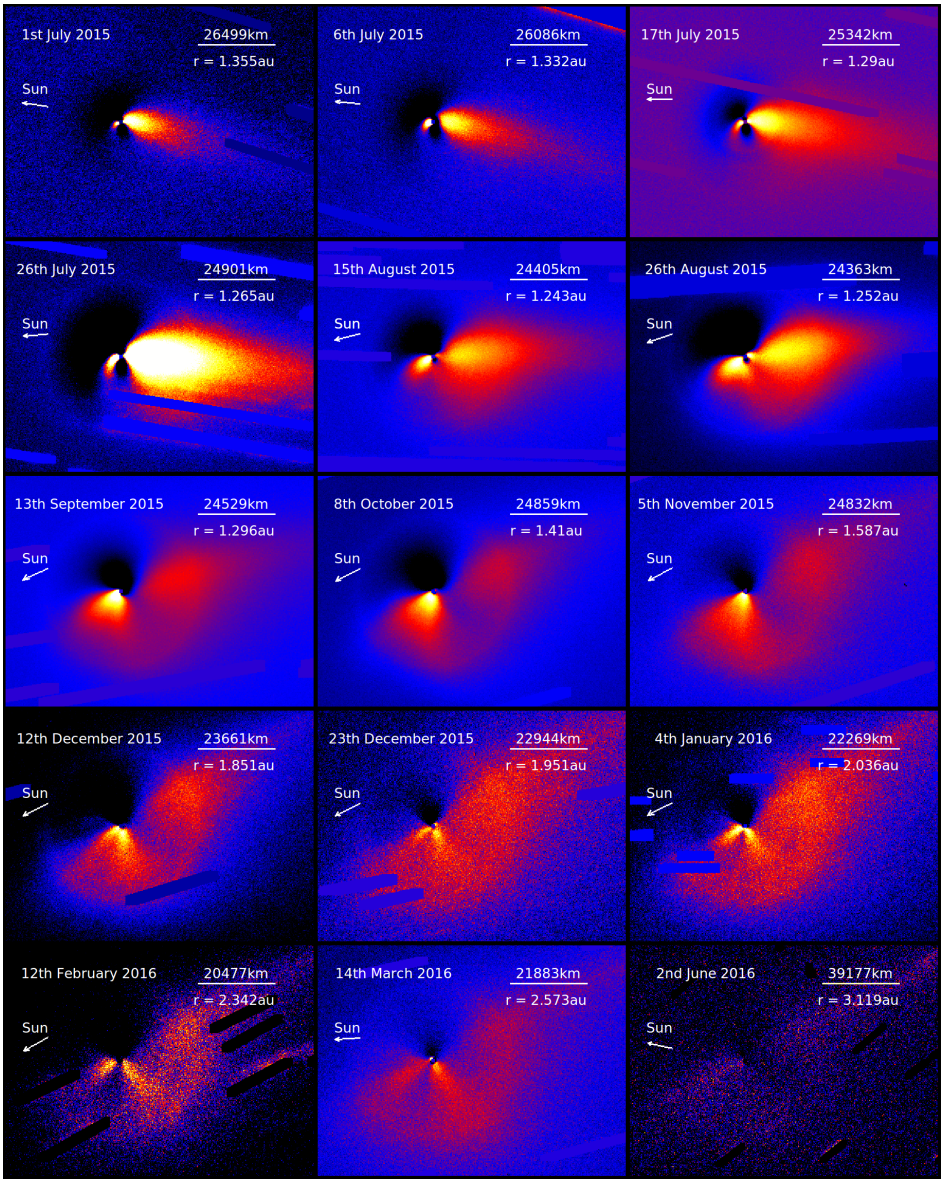

Figure 6.5: Morphology changes in the coma of comet 67P/C-G during our observation program with the NOT, published in paper IV. The contrast of the morphological features is enhanced by subtracting the azimuthally averaged profile of the coma. Dark stripes are background stars that have been masked out. The absolute brightness scales are heavily dependent on the observing conditions and therefore not directly comparable.

try, as the orientation of the comet's rotational axis is measured to great precision by the Rosetta spacecraft (Preusker et al. 2015).

No cometary coma is spherically symmetrical, although in some cases it can be quite close to such. There are several effects that break the symmetry. The activity on the cometary nucleus is biased towards the regions that receive most of the insolation and, therefore, produce a denser coma above. These tend to be localized around the equatorial regions, if the rotational axis of the nucleus is not strongly tilted, or around the summer side regions, if the tilt is significant. This, in turn, causes seasonal variations in coma structure, as discovered for comet 67P/C-G (see paper IV).

Sudden outbursts and other forms of uneven activity modulate the shape and brightness of the inner coma. Beside the obvious strong burst-like activities that can produce sharp jets spiraling out from the nucleus (Schulz et al. 2000), the day-night circle modulation of cometary activity can be one of the significant effects. In the case of comet 67P/C-G, Vincent et al. (2016) reported the "clockwork repeatability" of the appearance time of the small jets in the post-perihelion activity observed by Rosetta. This effect may have altered the coma structure by leaving the night side of the coma faint.

Matter in the outer coma is strongly affected by the solar radiation. If we have a reasonable estimate for the average particle velocity in the jet, we can use the curvature of the jet to calculate the radiation pressure sensitivity of the dust particles and, therefore, make some conclusions about the dust size distribution, albedo and average density. In reverse, if we have an estimate for the radiation pressure sensitivity of the dust particles, we can calculate the average dust velocity in the jet. Such an analysis was performed by Boehnhardt et al. (2016), with the resulting velocities greatly exceeding Rosetta's measurements (Della Corte et al. 2016). This discrepancy between Rosetta's inner coma measurements and the ground-based observations still warrants further research, as does the dust size distribution problem mentioned above.

Chapter 7

Discussion

This work consists of the four articles with a common research object, comet 67P/C-G. The methodological approach is, however, very different in each article. While papers II and IV present the main results of ground based optical observations with the NOT, papers I and III directly address *in-situ* data obtained by the COSIMA instrument onboard Rosetta.

The COSIMA data provided us with a unique chance to study cometary dust under the microscope and the mass spectrometer *in-situ*. Paper III describes the results of the visual inspection of the COSISCOPE images of the dust collected in the proximity of the active nucleus. Some results were surprising, such as the excessive fluffiness of the grains. The dust of comet 67P/C-G seems to be dominated by porous material which accounts for 75% of the total volume. The size distribution of the collected dust could not be fitted by a single power law, but rather appeared to have separate distributions for several size ranges. Particles larger than 150μm appear to approximatively follow the power law $r^{-0.8\pm0.1}$, while for the medium sized grains (30μm to 150μm) the relation would be $r^{-1.9\pm0.3}$. Dust particles below 30μm seem to have a flat cumulative size distribution. Paper I, in turn, describes the statistical analysis tool developed for the TOF-SIMS data of the COSIMA instrument which helps us to effectively study the chemical content of the grains. Routines based on these methods are currently used in the analysis of COSIMA spectra and will aid the research in the future.

Ground based optical observations represent the other part of this work. Papers II and IV present the two datasets acquired with the NOT using the same instruments and a similar observation strategy, but separated in time by the Solar conjunction. These datasets are, however, qualitatively differ-

ent. In the first block of data, the target appeared as a distant object with an unresolved structure, allowing us to perform photometry and astrometry, in addition to the partly successful attempt to resolve the brightness of the extended coma from the brightness of the point-like nucleus. From this work we can detect the start and the gradual increase of the activity with the reducing distance to the Sun, and define the lightcurve of the comet. In the post-conjunction data, the extended coma appeared in its full glory, allowing us to monitor changes in its structure and morphological features. The characteristic asymmetrical structure of the coma was qualitatively described as being seasonal and its origins were explained as the main result of paper IV. The photometric analysis of the post-conjunction observations is yet to be performed and will be one of the primary tasks of future work.

The possibility of combining *in-situ* and ground based approaches in order to correctly interpret observed phenomena is emphasized in this work. This was successfully performed in paper IV, where the orientation of the spin axis and the location of the activity regions of comet 67P/C-G, observed by the Rosetta instrumentation (Preusker et al. 2015; Vincent et al. 2016), were used to reconstruct and qualitatively describe the peculiar morphological features of the coma as seen from the ground.

Further attempts to combine Rosetta data with the ground based approach will guide the direction of future work. The most obvious goal is the comparison of the dust size distribution obtained *in-situ* by the Rosetta dust instruments COSIMA and GIADA (see paper III) to the estimates based on the modeling of the scattering processes of light observed from the ground. At the moment, the results disagree. According to paper III, the dust collected by COSIMA has a flat size distribution for particles below 30μm in diameter. However, in order to explain the scattering efficiency, a large amount of smaller particles is required (Fink & Rinaldi 2015). While it is obvious that the limited resolution of COSISCOPE does not allow us to resolve individual grains under 14μm in diameter, indirect evidence of their presence should have been detected. This discrepancy might be explained by the biased collection of the dust particles by Rosetta's instruments, or by the evolution of the dust size distribution as it propagates out of the innermost coma. For example, a significant role in both the dust collection bias and the fragmentation of dust may be assigned to electrostatic processes, as described by Horanyi et al. (2017).

Another interesting analysis could be the correlation between the comet's total activity level, acquired from the photometry of the ground based observations, and the magnitudes and frequencies of the local outbursts seen by the Rosetta spacecraft. In particular, the photometry of the NOT observations of the post-conjunction stage could be connected with the Rosetta data to reveal more details about the comet's activity and the propagation of dust to the outer coma.

Finally, many critical dust parameters measured *in-situ*, such as chemical composition, tensile strength, albedo and porosity, could be incorporated into the quantitative description of the behavior of cometary dust observed from the ground. For example, the Solar wind sensitivity of dust grains often has to be assumed or included as a parameter in the results in order to describe the curved cometary jets. Thus, comet 67P/C-G could be an ultimate test laboratory due to the independent measurements provided by Rosetta. Many phenomena, such as the morphological structure of the coma of comet 67P/C-G, described in paper IV, could also be observed at other comets. The processes can be reverse-engineered using Rosetta's experience, and previously unknown parameters can be derived for a large ensemble of comets unreachable for space missions.

Chapter 8

Summary of publications

8.1 Paper I: Analysis of COSIMA spectra: Bayesian approach.

In this work, a new method for the analysis of COSIMA TOF-SIMS data is presented. The typical mass spectra of the instrument have rather low statistics and a poor signal-to-noise ratio for each spectral line, which sets strong requirements for data analysis routines. In the method described in the paper, a Bayesian approach was employed in order to fit the proper model for signal peaks in the mass spectra. Using this routine, the mass resolution of weak signals can be enhanced and biased estimates avoided. The program is also able to resolve partly overlapping peaks, which provides a proper statistical way of defining the error limits and inference between the single- and the multiple-peak models.

The main idea of the method is to combine the Poisson distribution of the intrinsic noise of the individual datapoints (ion counts at each discretized unit of the time-of-flight scale) and estimate the global posterior distribution for each plausible model for the ion peak in the mass spectra. The main parameters of the model, such as the amplitude, position and shape of the peak, can be constrained and the confidence intervals defined. A posterior distribution of the model is mapped using MCMC methods combined with the Adaptive Metropolis algorithm. The resulting data analysis programs are currently used to investigate COSIMA spectra of the cometary grains captured in the coma of comet 67P/C-G during Rosetta's activity period.

8.2 Paper II: Optical observations of comet 67P/-Churyumov-Gerasimenko with the Nordic Optical Telescope. Comet activity before the solar conjunction.

This paper presents the first results of the ground-based observations with the Nordic Optical Telescope in support of the Rosetta mission. The regular observations started before Rosetta's rendezvous with comet 67P/C-G, which imposed a special role on the monitoring program regarding mission security. The comet was carefully monitored for any kind of unexpected activity or deviations from its predicted orbital path. Observed images were reduced and calibrated using standard routines, and the comet's positions were compared to the orbital predictions provided by the Minor Planet Center. The photometry of 67P/C-G was performed by comparing the brightness of the target with the measured brightness of catalog stars in the same field of view. Later, after the arrival of the Rosetta spacecraft at the comet, ground-based observations were used as a source of data complementary to Rosetta's measurements. The local activity variations observed on Rosetta's scales at a close proximity of the comet's nucleus were compared with the statistically averaged global activity observed from the ground.

The target was successfully monitored during the period between the 12th of May 2013 and the 11th of November 2014, until the invisibility period caused by the Solar Conjunction. The main results of the paper were general confirmations of both the orbital predictions of the astrometric location of the comet and the predicted development of the activity, apart from the minor fading observed in late September 2014 (see Figure 6.3). The sudden ignition of the comet's activity was observed in April 2014 at the heliocentric distance of 4.11 AU, which appeared as a rise in the overall brightness and the emergence of the extended coma. The deviation from the point-source profile was further investigated using Bayesian statistics, and constraints on the spatial size and brightness contribution of the coma in several observations were estimated.

8.3 Paper III: Dust particle flux and size distribution in the coma of 67P/Churyumov-Gerasimenko measured in situ by the COSIMA instrument on board Rosetta.

This work presents the statistical properties of the cometary dust particles obtained with the COSIMA instrument onboard Rosetta during the period between the 11th of August 2014 and the 6th of April 2015. The results are deduced from direct *in-situ* data and therefore provide a good complementary source of information for meta-analytical studies. The dust particles were examined using an optical microscope (COSISCOPE) after each exposure period, which provided daily to weekly time resolutions. By the time of the publication, more than 10000 cometary dust particles had been collected by COSIMA. The visual inspection of those particles divided them into two categories: compact particles and porous aggregates. The texture of the porous particles looks similar to the chondritic porous IDP:s collected in the Earth's atmosphere and corresponds to 75% of the total volume of the collected dust. The dust flux seems to be heavily dominated by large outbursts, during which most of the dust was collected. It may be, therefore, insufficient to merely assume a steady uplift of dust from the surface of the nucleus with averaged gas outflow velocities.

One of the key results of this work is the cumulative size distribution of the dust particles which shows a power-law dependence with the relation $N(r) \approx r^{-1.69}$ to $r^{-2.17}$ for particles smaller than 100μm and $N(r) \approx r^{-0.78}$ for particles larger than that. The distribution of the dust particles contradicts some other estimates obtained with different techniques (Moreno et al. 2016), which may indicate that the dust collection of the COSIMA instrument is biased towards grain sizes between 10 μm and 100 μm. There is also no evidence of the presence of the large amount of fine dust expected from the light scattering processes (Fink & Rinaldi 2015). The resolution of COSISCOPE is insufficient for the individual detection of such particles and further investigations must rely on indirect methods, such as the alteration of substrate albedo or the cometary signals in the TOF-SIMS data.

8.4 Paper IV: Solar-insolation-induced changes in the coma morphology of comet 67P/Churyumov-Gerasimenko. Optical monitoring with the Nordic Optical Telescope.

In this paper, a new discovery of the seasonal variations in the coma morphology for comet 67P/C-G is published. The morphological features observed from the ground with the Nordic Optical Telescope were correlated with the distribution of local outbursts on the nucleus observed with Rosetta (Vincent et al. 2016). Using simple physical models, the clear connection between the start of the activity on the southern hemisphere of the comet's nucleus and the alteration of the morphology of the coma was established. Similar effects of changing coma morphology have been observed in comets before, and the effects of seasonal changes were suspected (Sekanina 1988). However, in this work we have clear evidence of this phenomenon, thanks to the supportive data from the Rosetta spacecraft.

The paper utilizes simplified modeling of the coma density distribution in space, using a finite element approach. In this method, a three-dimensional array was used to represent evenly spaced subunits. The value of each point of an array represents the local density of the coma and hence also the amount of scattered light. The scattering properties of the dust particles are assumed to be uniform throughout the coma, as the examination of the differential images obtained by the subtraction of the normalized V-band image from the R-band image showed a lack of color gradients.

The main result of the paper is the qualitative description of the processes altering coma morphology and their connection to the seasonal changes in the insolation of the nucleus surface. The changes, however, appeared with a time delay of several weeks with respect to the series of outbursts observed by Rosetta. This may be connected to the uneven activity of the austral regions which presumably distorted the morphological features. Another interesting observation was the greatly reduced activity of the northern hemisphere which used to be more active during the previous apparitions of comet 67P/C-G (Vincent et al. 2013). Similar processes may be expected to occur in other comets if equivalent morphology structures are observed.

Appendix A

Astrometric solution table

Table A.1: Astrometric Solution Results for 67P/C-G before the detection of comet by the Rosetta spacecraft. The coordinates α(J2000.0) and δ(J2000.0) include horizontal parallax specific for the location of the NOT. The error limits of 3σ are presented in the two last columns and combine the target location error with the astrometric calibration errors.

Date	UT	α(J2000.0)	δ(J2000.0)	$\Delta\alpha$	$\Delta\delta$
2013 05 13	02:20:38.10	17:46:43.34	-27:24:59.18	0.80”	0.80”
2013 05 13	02:26:03.13	17:46:43.56	-27:24:59.47	0.80”	0.81”
2013 06 02	02:57:50.39	17:23:42.51	-27:31:17.01	0.63”	0.62”
2013 06 02	03:03:14.82	17:23:42.33	-27:31:17.01	0.60”	0.61”
2013 06 02	03:08:39.15	17:23:42.18	-27:31:17.02	0.60”	0.61”
2013 06 02	03:14:03.51	17:23:42.00	-27:31:17.01	0.62”	0.62”
2013 06 02	03:19:27.90	17:23:41.82	-27:31:17.00	0.61”	0.61”
2013 08 13	21:15:31.39	16:44:12.30	-26:38:23.13	0.61”	0.61”
2013 08 27	03:08:39.15	16:44:12.57	-26:31:46.73	0.47”	0.48”
2013 08 27	20:50:36.57	16:44:12.67	-26:31:46.16	0.47”	0.48”
2013 08 27	20:56:01.61	16:44:12.70	-26:31:45.95	0.47”	0.48”
2014 03 05	06:03:31.30	19:18:31.68	-26:51:45.50	0.80”	0.81”
2014 03 05	06:07:16.47	19:18:31.90	-26:51:45.28	0.81”	0.81”
2014 03 05	06:11:01.66	19:18:32.17	-26:51:44.94	0.80”	0.81”
2014 03 05	06:14:46.66	19:18:32.39	-26:51:44.79	0.80”	0.81”
2014 03 05	06:18:32.06	19:18:32.63	-26:51:44.66	0.80”	0.81”
2014 03 12	05:39:52.80	19:24:27.45	-26:49:14.33	0.79”	0.80”
2014 03 20	05:39:13.70	19:30:37.22	-26:46:47.54	0.79”	0.80”
2014 04 05	04:56:05.90	19:41:06.75	-26:46:39.95	0.63”	0.63”
2014 04 05	05:34:34.70	19:41:05.80	-26:46:39.95	0.42”	0.42”

Author's contribution to the publications

Paper I: Analysis of COSIMA spectra: Bayesian approach.
The author is responsible for part of the development and testing of the software, application and implementation of the mathematical methods and preparing part of the manuscript, covering 50% of the total amount of work.

Paper II: Optical observations of comet 67P/Churyumov-Gerasimenko with the Nordic Optical Telescope. Comet activity before the solar conjunction.
The author is responsible for the planning of the observations, data reduction, analysis and writing, covering most (95%) of the total amount of work.

Paper III: Dust particle flux and size distribution in the coma of 67P/Churyumov-Gerasimenko measured in situ by the COSIMA instrument on board Rosetta.
The author is responsible for the statistical analysis of the spatial distributions of the collected dust, as well as for writing the chapter covering this subject. The author's contribution covers approximately 10% of the total amount of work.

Paper IV: Solar-insolation-induced changes in the coma morphology of comet 67P/Churyumov-Gerasimenko. Optical monitoring with the Nordic Optical Telescope.
The author is responsible for half of the standard image reduction and for the rest of the data analysis and preparing of the manuscript, covering 90% of the total amount of work.

Bibliography

Aad, G., Abajyan, T., Abbott, B., et al. 2012, Physics Letters B, 716, 1

Agarwal, J., Müller, M., Reach, W. T., et al. 2010, Icarus, 207, 992

Altwegg, K., Balsiger, H., Bar-Nun, A., et al. 2015, Science, 347, 1261952

Arpigny, C. 1965, ARA&A, 3, 351

Biele, J., Ulamec, S., Maibaum, M., et al. 2015, Science, 349

Bieler, A., Altwegg, K., Balsiger, H., et al. 2015a, Nature, 526, 678

Bieler, A., Altwegg, K., Balsiger, H., et al. 2015b, A&A, 583, A7

Boehnhardt, H., Riffeser, A., Kluge, M., et al. 2016, MNRAS, 462, S376

Brownlee, D. 2014, Annual Review of Earth and Planetary Sciences, 42, 179

Calabretta, M. R. & Greisen, E. W. 2002, A&A, 395, 1077

Davidsson, B. J. R., Sierks, H., Güttler, C., et al. 2016, A&A, 592, A63

de Vaucouleurs, G. 1958, ApJ, 128, 465

Della Corte, V., Rotundi, A., Fulle, M., et al. 2016, MNRAS, 462, S210

Fernandez, J. 2006, Comets: Nature, Dynamics, Origin, and their Cosmogonical Relevance, Astrophysics and Space Science Library (Springer Netherlands)

Fink, U. & Rinaldi, G. 2015, Icarus, 257, 9

Fray, N., Bardyn, A., Cottin, H., et al. 2016, Nature, 538, 72

Gelman, A., Carlin, J. B., Stern, H. S., & Rubin, D. B. 2004, Bayesian data analysis, 2nd edn., Texts in Statistical Science Series (Chapman & Hall/CRC, Boca Raton, FL), xxvi+668

Grün, E., Agarwal, J., Altobelli, N., et al. 2016, MNRAS, 462, S220

Hilchenbach, M., Kissel, J., Langevin, Y., et al. 2016, ApJ, 816, L32

Horanyi, M., Deca, J., Gruen, E., & Havnes, O. 2017, in EGU General Assembly Conference Abstracts, Vol. 19, EGU General Assembly Conference Abstracts, 9800

Hornung, K., Merouane, S., Hilchenbach, M., et al. 2016, Planet. Space Sci., 133, 63

Huebner, W. 1990, Physics and Chemistry of Comets, Astronomy and Astrophysics Library (Springer Berlin Heidelberg)

Jenniskens, P. 2006, Meteor Showers and their Parent Comets

Jones, G. H., Knight, M. M., Fitzsimmons, A., & Taylor, M. G. G. T. 2017, Philosophical Transactions of the Royal Society of London Series A, 375, 20170001

Keller, H. U., Arpigny, C., Barbieri, C., et al. 1986, Nature, 321, 320

Kissel, J., Altwegg, K., Clark, B. C., et al. 2007, Space Sci. Rev., 128, 823

Knight, M. M. & Battams, K. 2014, ApJ, 782, L37

Kolokolova, L., Koenders, C., Goetz, C., et al. 2016, MNRAS, 462, S422

Krankowsky, D., Lammerzahl, P., Herrwerth, I., et al. 1986, Nature, 321, 326

Lamy, P. L., Toth, I., Weaver, H. A., et al. 2006, A&A, 458, 669

Lara, L.-M., Tozzi, G. P., Boehnhardt, H., DiMartino, M., & Schulz, R. 2004, A&A, 422, 717

Maquet, L. 2015, A&A, 579, A78

Mayo Greenberg, J. & Mendoza-Gómez, C. X. 1992, Advances in Space Research, 12, 169

Moreno, F., Snodgrass, C., Hainaut, O., et al. 2016, A&A, 587, A155

Mottola, S., Lowry, S., Snodgrass, C., et al. 2014, A&A, 569, L2

Mour, R. R. D. 2009, in Astronomical Society of the Pacific Conference Series, Vol. 409, Cosmology Across Cultures, ed. J. Rubiño-Martín, J. Belmonte, F. Prada, & A. Alberdi, 297

Pajola, M., Höfner, S., Vincent, J. B., et al. 2017, Nature Astronomy, 1, 0092

Pätzold, M., Andert, T., Hahn, M., et al. 2016, Nature, 530, 63

Preusker, F., Scholten, F., Matz, K.-D., et al. 2015, A&A, 583, A33

Rickman, H., Marchi, S., A'Hearn, M. F., et al. 2015, A&A, 583, A44

Saksman, E. & Vihola, M. 2008, ArXiv e-prints

Schulz, R., Stüwe, J. A., Tozzi, G. P., & Owens, A. 2000, A&A, 361, 359

Sekanina, Z. 1988, AJ, 96, 1455

Sekanina, Z. & Yeomans, D. K. 1984, AJ, 89, 154

Sierks, H., Barbieri, C., Lamy, P. L., et al. 2015, Science, 347, aaa1044

Snodgrass, C., Tubiana, C., Bramich, D. M., et al. 2013, A&A, 557, A33

Stoyan, R. & Dunlop, S. 2015, Atlas of Great Comets (Cambridge University Press)

Szydlik, P. P. & Flynn, G. J. 1992, Meteoritics, 27

Tamminen, J., Haario, H., Kyrola, E., Oikarinen, L., & Saksman, E. 1998, in Proc. SPIE, Vol. 3439, Earth Observing Systems III, ed. W. L. Barnes, 470–479

Tody, D. 1986, in Proc. SPIE, Vol. 627, Instrumentation in astronomy VI, ed. D. L. Crawford, 733

Van Nouhuys, T. 1998, The Ages of Two-faced Janus: The Comets of 1577 and 1618 and the Decline of the Aristotelian World View in the Netherlands, Brill's studies in intellectual history / Brill's studies in intellectual history (Brill)

Vincent, J.-B., A'Hearn, M. F., Lin, Z.-Y., et al. 2016, MNRAS, 462, S184

Vincent, J.-B., Lara, L. M., Tozzi, G. P., Lin, Z.-Y., & Sierks, H. 2013, A&A, 549, A121

Weiler, M., Rauer, H., & Helbert, J. 2004, A&A, 414, 749

Whipple, F. L. 1950, ApJ, 111, 375